Unsupervised Morphological Multiscale Segmentation of Scanning Electron Microscopy Images

Gianni Franchi, Jesus Angulo, Maxime Moreaud

UNSUPERVISED MORPHOLOGICAL MULTISCALE SEGMENTATION OF SCANNING ELECTRON MICROSCOPY IMAGES

Gianni Franchi[⋆] *Jesús Angulo*[⋆] *Maxime Moreaud*[†]

[⋆] CMM-Centre for mathematical morphology, MINES Paristech, France
[†] IFP Energies nouvelles, Solaize, France

ABSTRACT

This paper deals with a problem of unsupervised multiscale segmentation in the domain of scanning electron microscopy, which is tackled by mathematical morphology techniques. The proposed approach includes various steps. First, the image is decomposed into various compact scales of representation, where objects at each scale are homogeneous in size. Multiscale decomposition is based on a morphological scale-space followed by scale merging using hierarchical clustering and earth mover distance. Then the compact scales are segmented independently using watershed transform. Finally the segmented scales are combined using a tree of objects in order to obtain a multiscale segmentation.

Index Terms— multiscale segmentation, morphological scale-space, watershed algorithm

1. INTRODUCTION

A scanning electron microscope (SEM) is a microscope that produces images thanks to a focused beam of electrons. The interactions between the electrons and the sample can produce different modalities of images [1]. In this study we focus on images acquired using backscattered electrons mode, which is mainly used to enhance information about the sample composition, see two examples in Fig. 1.

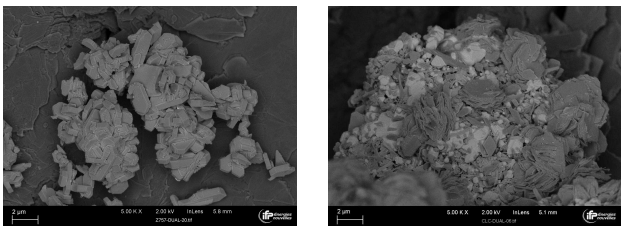

Fig. 1. Two examples of backscattered electron mode SEM images.

The purpose of the paper is to explore innovative techniques from mathematical morphology to improve the automatic segmentation of the "active phase" in SEM images, which can be observed in examples of Fig. 1 as the bright structures. Mathematical morphology is widely used for image segmentation in material science microscopy imaging [2, 3, 4].

From the image processing viewpoint, it is necessary to segment and quantify the structures of the active phase, in order to compute for instance the distribution of size and shape. Also unsupervised techniques are crucial to perform automated high-throughput SEM imaging process. The main difficulty for a such unsupervised segmentation is the fact that the active phase can appears at different scales in the same image (i.e., small or very large objects) and at different intensity distributions. By the way, a simple segmentation approach based on thresholding is not appropriate since we need to individually separate each grain/object. This kind of multiscale segmentation problem can be solved using different paradigms. In particular, mathematical morphology provides hierarchical segmentation approaches adapted to that purpose [5, 6, 7]. The classic idea is to first build a hierarchial partition of the image and second to find an optimal cut in the hierarchy which represents properly the different scales, see for instance the recent approach [8].

We adopt here a different multiscale segmentation paradigm summarized in the diagram of Fig. 2, which involves four steps discussed in Section 3. The fundamental different of our multiscale algorithm with respect to the classical hierarchial approaches is the fact that we first perform a compact multiscale image decomposition, used next for building the hierarchical tree, which is finally simplified by a straightforward pruning approach.

2. NOTATIONS AND BASIC NOTIONS

Let E be a subset of the discrete space $\mathbb{Z}^2$, which represents the support space of a 2D image and $\mathcal{T} \subseteq \mathbb{R}$ be the set of intensity pixels values. Hence, it is assumed that the value at a pixel position $x \in E$ is represented by a scalar grey-level intensity $s \in \mathcal{T}$ by means of the function $f : E \to \mathcal{T}$.

Morphological opening of f according to structuring element B is defined as $\gamma_B(f) = \delta_B(\varepsilon_B(f))$, where $\varepsilon_B(f)$ and $\delta_B(f)$ are respectively the erosion and the dilation of f by

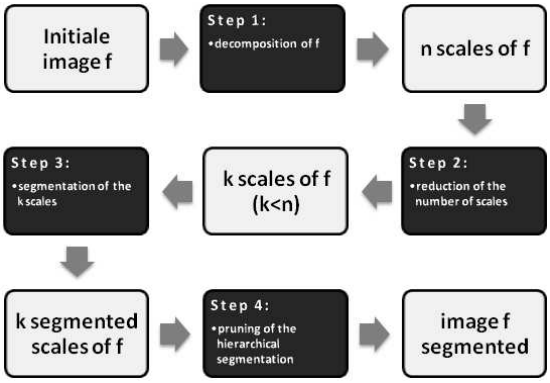

Fig. 2. The process of multiscale segmentation in four steps.

the flat structuring element B [9]. More generally, an algebraic opening $\gamma(f)$ is any operator on f following these three properties [9]: (a) increasing, i.e., if $f \leq g$ then $\gamma(f) \leq \gamma(g)$; (b) idempotent, i.e., $\gamma(\gamma(f)) = \gamma(f)$; (c) anti-extensive, i.e., $\gamma(f) \leq f$. The latter property means that bright structures are removed from the image. Similarly, an algebraic closing φ is any operator $\mathcal{F}(E,\mathcal{T}) \rightarrow \mathcal{F}(E,\mathcal{T})$ being increasing, idempotent and extensive (i.e., acting on dark structures).

Area opening (resp. area closing) is a morphological filter that removes from an image the bright (resp. dark) connected components having a surface area smaller than the parameter λ [10]. Area openings on gray-level images can be implemented from an upper level set decomposition as well as using more efficient algorithms based on max-tree [11] or component tree [12] representations. For a recent overview of applications of area openings, see [13]. It is also possible to formulate area-based operators which simultaneously filter out bright and dark connected components and consequently being self-dual [14]. The same effect can be obtained by working a tree representation of the image called Fast Level Lines Transform [15]. The main interest of area opening resides in the fact that they can be seen as morphological openings with a structuring element which locally adapts its shape to the image structures and consequently the contours of the objects are not deformed.

Area opening is a typical example of algebraic opening. Given a binary image b, which can be represented by the set of the finite union of its connected components of value 1, i.e., $\mathcal{C}_b^+ = \cup_k C_k$ such that $b\left(\{C_k\}\right) = 1$, the area opening of size $0 < \lambda \in \mathbb{N}$ is defined as follows [10]:

$$\gamma_\lambda(b) = \bigcup_k \{C_k | \text{area}(C_k) \geq \lambda\}. \tag{1}$$

Therefore, $\gamma_\lambda(b)$ is the union of the connected components of b with area greater or equal than λ. By area is meant the Lebesgue measure in $\mathbb{Z}^2$.

Area openings are naturally extended to grey-scale images [10]. Since we are going to work on the connected components of grey-scale image $f \in \mathcal{F}(E,\mathcal{T})$, it is common to decompose it into its upper level sets, where the upper level set for a given threshold $s \in \mathcal{T}$ and a given image f is the binary image defined as:

$$X_s(f)(x) = \begin{cases} 1 \text{ if } f(x) \geq s \\ 0 \text{ if } f(x) < s \end{cases} \tag{2}$$

Using now the family of upper level set, we can easily obtain the original image as [16]: $f = \sum_{s\in\mathcal{T}} X_s(f)$. If we have defined the binary area opening Γ_λ with the attribute value λ, the corresponding grey-scale area opening γ_λ of image f is given by

$$\gamma_\lambda(f) = \sum_{s\in\mathcal{T}} \Gamma_\lambda(X_s(f)). \tag{3}$$

3. THE ALGORITHM

3.1. Step 1: Morphological multiscale decomposition

Let us consider $\{\gamma_i\}_{1\leq i\leq n}$ an indexed family of area openings. Thus, the scale index i is associated to the size of the area. Morphological decomposition by the family $\{\gamma_i\}_{1\leq i\leq n}$ is related to the notion of granulometry [9]. Namely, we have two fundamental axioms: i) ordering $\gamma_n(f) \leqslant \gamma_{n-1}(f) \leqslant \ldots \leqslant \gamma_2(f) \leqslant \gamma_1(f) \leqslant f$; and ii) semi-group law $\gamma_i(\gamma_j(f)) = \gamma_j(\gamma_i(f)) = \gamma_{\sup(i,j)}(f)$, $1 \leq i,j \leq n$. By convention, we define $\gamma_0(f) = f$. Using this nonlinear scale-space schema, we have now the following image decomposition [17]:

$$f = \sum_{i=1}^{n} (\gamma_{i-1}(f) - \gamma_i(f)) + \gamma_n(f) \tag{4}$$

By defining the residue at scale i as follows: $R_i(f) = \gamma_{i-1}(f) - \gamma_i(f)$, such that $R_i(f)(x) \geq 0$, $\forall x \in E$, one can now rewrite Eq.(4) as

$$f = \sum_{i=1}^{n} R_i(f) + \gamma_n(f) = R(f) + \gamma_n(f) \tag{5}$$

Therefore we have a decomposition of the initial image f into n scales, together with the last area opening. We remark that the residue R_i represents the difference between an image where we keep all structures of area larger than $i-1$ and another one where structures of area larger than i are preserved. In other words, this residue stands for structures of area between levels i and $i-1$. Hence the set $\{R_1, \ldots, R_n\}$, constitutes in a way a hierarchy of area-based multiscale morphological components. However by decomposing an image into scales we have now to deal with an object of bigger dimensionality, moreover the decomposition is not optimal: it depends on the discretization into n scales, the size of scale, etc.

3.2. Step 2: Reducing multiscale decomposition

Decomposition represented by $\{R_i\}_{1\leq i\leq n}$ needs to be "compacted". That involves reducing the dimensionality of the hierarchy (i.e., reducing the number of scales to k), according to three main criteria:

C1: a new scale has only objects of similar size;

C2: to loss as less information as possible, such as one has a good approximation to decomposition (5) with $k < n$;

C3: hierarchy has to be as sparse as possible.

C2 and C3 can be addressed as an optimisation problem that can be handled for instance by PCA or its sparse variants. However, such approaches do not optimise the criterion C1. Therefore we formulate this problem as a case of unsupervised classification, aiming at clustering the residues in order to decrease the number of classes. In any case, we first use PCA to estimate the dimensionality of the hierarchy and thus to choose the number of reduced scales k.

For our unsupervised classification, we used Hierarchical Ascendant Classification (HAC), with the additional constrain that only adjacent scales can be merged. By this approach we guarantee that criterion C1 holds. Then, we have that:

$$\{R_i(f)\}_{i=1}^{n} \longrightarrow^{HAC} \{S_j(f)\}_{j=1}^{k} \tag{6}$$

where $S_j(f) = \sum_{i=l_j}^{l_{j+1}-1} R_i(f)$ such that l_j is the first initial scale associated to class j of our HAC.

Obviously, the main ingredient in HAC is the similarity criterion between residues. We have evaluated several alternatives: Earth Mover Distance (EMD)[18] [19], Kullback-Leibler Distance, Entropy, Hausdorff Distance and Correlation. Based on a study which compared the performance of these similarity criteria (results not included by limited length of the paper), we obtained that EMD outperforms the other techniques.

From EMD-based HAC, we still have a full reconstruction of the initial image, i.e., $f = \sum_{j=1}^{k} S_j(f) + \gamma_n(f)$. Initial scales can be contaminated by "noise" which will be also present in the compact scales. Filtering this noise can be seen as aiming at a more sparse representation, which is related to C3. Introducing sparsity on the hierarchy involves to force to zero as much elements as possible in $\{S_j\}_{1\leq j\leq k}$. This goal is achieved in two steps: i) shrinkage/thresholding since a noisy structure in S_j is an object having a very low grey-level, i.e., $S'_j = \{S_j \text{ if } abs(S_j) > \alpha;\ 0 \text{ otherwise}\}$ and ii) size filtering since a noisy structure in S_j is an object having a size significantly small with respect to the typical size of the scale j, i.e., $S''_j = \gamma_{B_{j/2}}\left(S'_j\right)$. Finally, after these processing steps, we have a decomposition given by $\{S''_j\}_{1\leq j\leq k}$ and thus an appropriate approximation of the initial image:

$$f \approx \sum_{j=1}^{k} S''_j(f) + \gamma_n(f). \tag{7}$$

3.3. Step 3: Segmentation of the multiscale decomposition

After having gathered the different scales (dimensionality reduction) and filtered out the noise (forcing sparseness), the improved hierarchy $\{S''_j\}_{1\leq j\leq k}$ is ready to be segmented, scale by scale. To perform it, we applied a marked watershed transform [20] on each scale. More precisely, the morphological gradient of each image $S''_j(f)$ is computed which is then used as the flooding function for the watershed. Consequently, a region (or class of the partial partition of the image space) is obtained for each local minimum presents in the gradient of $S''_j(f)$. We note that $\gamma_n(f)$ is in a way the background of the image, which is not useful for the segmentation of the relevant structures.

As we can see from Fig. 3, we have the segmented images (for this example $k = 7$, starting from $n = 20$). From the example we note that the multiscale segmentation is redundant since image structures are present in various scales. That means that sometimes the watershed transform detects different objects whereas there is just one, and sometimes the contrary situation. By the way, we have k partitions and our aim is to provide a single multiscale one by merging the k segmentations.

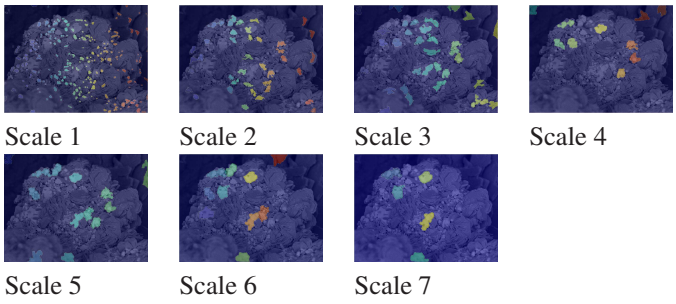

Fig. 3. Result of a marker-based watershed on each scale.

3.4. Step 4: Hierarchical segmentation

The $S''_j(f)$ represents the level of approximation of scale j and consequently, we can write

$$\tilde{f} = \sum_{j=1}^{k} S''_j(f) \tag{8}$$

where $\tilde{f}$ represents all the relevant image structures to be segmented. Now, using the k partitions, we create a tree that links each object from $\tilde{f}$ with its corresponding sons at each level of detail j, for all $j \in [1, k]$, see Fig.4. To have a better understanding, let us consider that $\tilde{f}$ is segmented into N objects and each one is denoted by C_l, $l = 1 \ldots N$. We will write a son of C_l at the level of approximation j, by $C^l_{j,i}$ where i is the index of this son in comparison to all his brothers at

this level of approximation. Pruning this tree is rather simple since the cut for each C_l is done independently.

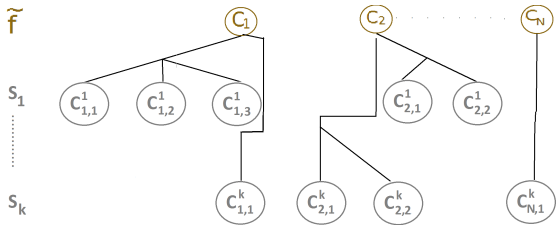

Fig. 4. A representation of a tree of optimal classes.

The cut is based on the following estimation technique. We compare for each segmentation level j the similarity between the raw object C_l and all its segmented sons $\{C^l_{j,i}\}_i$ at this level, and then we take the set of sons at the level j that are the better approximation to the father C_l. We have considered again different criteria to evaluate the similarity between C_l and $\{C^l_{j,i}\}_i$, such as the correlation, entropy Hausdorff distance, Kullback Leibler distance and EMD. In order to measure the optimality of each technique we have assessed them using a ground-truth manually segmented set of images (low false positive ratio and small false negative ration). We have also taken into account the time of computation. Overall, the technique based on the correlation best fit all the criteria.

4. RESULTS

We have applied the present multiscale segmentation algorithm to a selection of backscattered electron mode SEM images of different catalyst materials, some examples are given in Fig. 5.

We compared these results of this algorithm, with those of other hierarchical segmentation techniques, in particular with the approach of hierarchical cuts and climbing energies [8]. With this algorithm we had a false positive rate of 0.21 and an initial true positive rate of 0.85; whereas for the same example the approach [8] produces a true positive rate a bit weaker for the optimization energy we tried. Other energies in [8] can potentially outperform our results.

False positive rate can be reduced by changing the threshold α used in Step 2. The appropriate choice of α should be based on the ROC curve depicted in Fig. 6.

It is also important to note that the unique parameter of the algorithm is the initial discretization of the area opening-based decomposition. We have developed a strategy in order to fit an appropriate discretization for a given number of n scale. However this point is out of the scope of the paper.

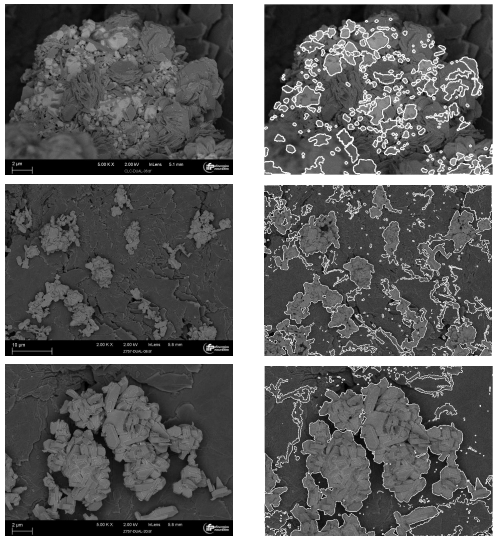

Fig. 5. Results of the multiscale segmentation of backscattered electron mode SEM images.

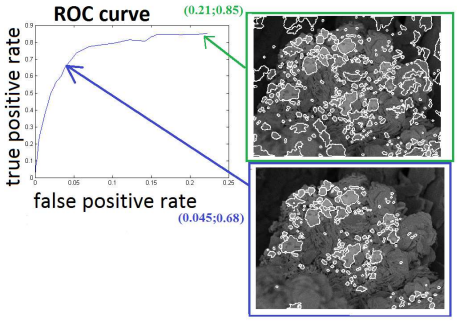

Fig. 6. ROC curve to determine detection threshold.

5. CONCLUSIONS

The purpose of the study was to explore innovative techniques from mathematical morphology to achieve a fully automatic multi-scale segmentation of SEM images. In order to perform it, we implemented a four steps algorithm illustrated in Figure 2. With respect to other generic hierarchical approaches of segmentation available in the state-of-the-art, we note that our algorithm starts with an image decomposition into compact homogenous scales of objects which involves that the final hierarchical structure is a very simple tree of objects where the merging step is managed independently for each zone of the image.

The approach has been evaluated in a representative database of images from backscattered SEM images and the results are very promising. As natural extension of this work, we are presently considering the generalization approach to the case of multi-modal SEM images.

6. REFERENCES

[1] L. Reimer, *Scanning Electron Microscopy, Physics of Image Formation and Microanalysis*, Series: Springer Series in Optical Sciences Vol. 45. 2nd completely rev. and updated ed., 1998.

[2] M. Faessel and D. Jeulin, "Segmentation of 3d microtomographic images of granular materials with the stochastic watershed," *Journal of Microscopy*, vol. 239, no. 1, pp. 17–31, 2010.

[3] L. Sorbier, A. S. Gay, A. Fécant, M. Moreaud, and N. Brodusch, "Measurement of palladium crust thickness on catalysts by optical microscopy and image analysis," vol. 19, pp. 293–299.

[4] M. Moreaud, D. Jeulin, A. Thorel, and J.Y. Chane-Ching, "A quantitative morphological analysis of nanostructured ceria–silica composite catalysts," *Journal of microscopy*, vol. 232, no. 2, pp. 293–305, 2008.

[5] F. Meyer, "Hierarchies of partitions and morphological segmentation," in *Scale-Space and Morphology in Computer Vision*, pp. 161–182. Springer Berlin Heidelberg, 2006.

[6] L. Najman and M. Schmitt, "Geodesic saliency of watershed contours and hierarchical segmentation," *IEEE Trans. Pattern Anal. Mach. Intell.*, vol. 18, no. 12, pp. 1163–1173, Dec. 1996.

[7] J. Angulo and D. Jeulin, "Stochastic watershed segmentation," in *Proc. of the 8th International Symposium on Mathematical Morphology (ISMM'2007)*. 2007, pp. 265–276, MCT/INPE.

[8] B.R. Kiran and J. Serra, "Global-local optimizations by hierarchical cuts and climbing energies," *Pattern Recogn.*, vol. 47, no. 1, pp. 12–24, Jan. 2014.

[9] J. Serra, *Image Analysis and Mathematical Morphology*, Academic Press, Inc., Orlando, FL, USA, 1983.

[10] L. Vincent, "Morphological area opening and closing for grayscale images," *Proc. NATO Shape in Picture Workshop, Driebergen, The Netherlands, Springer-Verlag*, pp. 197–208, September 1992.

[11] P. Salembier, A. Oliveras, and L. Garrido, "Anti-extensive connected operators for image and sequence processing," *IEEE Trans. Image Processing, vol. 7*, pp. 555–570, Apr. 1998.

[12] L. Najman and M. Couprie, "Building the component tree in quasi-linear time," *IEEE Trans. Image Processing, vol. 15, no. 11*, pp. 3531–3539, Nov. 2006.

[13] G. K. Ouzounis, M. Pesaresi, and P. Soille, "Differential area profiles: Decomposition properties and efficient computation," *Pattern Analysis and Machine Intelligence, IEEE Transactions on , vol.34*, pp. 1533–1548, Aug. 2012.

[14] P. Soille, "Beyond self-duality in morphological image analysis," *Image and Vision Computing, Volume 23, Issue 2*, pp. 249–257, February 2005.

[15] P. Monasse and F. Guichard, "Fast computation of a contrast-invariant image representation," *Image Processing, IEEE Transactions on , vol.9, no.5*, pp. 860–872, May 2000.

[16] P. Maragos and R.W. Schafer, "Morphological filters–part ii: Their relations to median, order-statistic, and stack filters," *Acoustics, Speech and Signal Processing, IEEE Transactions on , vol.35, no.8*, pp. 1170–1184, Aug 1987.

[17] S. Velasco-Forero and J. Angulo, "Classification of hyperspectral images by tensor modeling and additive morphological decomposition," *Pattern Recogn.*, vol. 46, no. 2, pp. 566–577, Feb. 2013.

[18] O. Pele and M. Werman, "Fast and robust earth mover's distances," in *Computer Vision, 2009 IEEE 12th International Conference on*, 2009, pp. 460–467.

[19] O. Pele and M. Werman, "A linear time histogram metric for improved sift matching," in *Proceedings of the 10th European Conference on Computer Vision: Part III*, Berlin, Heidelberg, 2008, ECCV '08, pp. 495–508, Springer-Verlag.

[20] F. Meyer and S. Beucher, "Morphological segmentation," *journal of visual communication and image representation 1 (1)*, pp. 21–46, 1990.